JOURNAL OF MATERIALS SCIENCE 18 (1983) 2510–2516

X-ray diffraction analysis at high temperature on two ceramic systems

A. BENEDETTI, G. FAGHERAZZI*
Istituto di Chimica Fisica, Università Cà Foscari, D.D.2137, 30123 Venezia, Italy
S. MERIANI
Istituto di Chimica Applicata, Università, via Valerio 2, 34127 Trieste, Italy

The β-eucryptite/β-spodumene phase transition in glass fibres of a SiO_2–Al_2O_3–Li_2O–MgO–ZnO–K_2O–P_2O_5 system and the crystallization of a ZrO_2–CeO_2 solid solution have been studied *in situ*, at high temperature, using a special home-made thermal attachment for X-ray powder vertical diffractometers. The β-eucryptite/β-spodumene transition was observed in the temperature range between 865 and 930° C. A significant unit cell shrinkage was observed for β-eucryptite from which it is possible to conclude that the first crystallized phase is surely an eucryptite-silica solid solution. This agrees with the small thermal effect shown by DTA for this crystalline transition. With the same high temperature attachment the evolution of the average crystallite size, L_{111}, was followed as a function of the thermal treatment in a 0.84 ZrO_2–0.16 CeO_2 tetragonal structured solid solution.

1. Introduction

In this paper the importance of X-ray diffraction analyses *in situ* at high temperature for the elucidation of the crystallization process of ceramic materials is shown with reference to two different examples.

A special home-made thermal attachment for X-ray powder vertical diffractometers was applied to study the following two ceramic systems: (i) glass fibres of composition (mol %): SiO_2 62.85, Al_2O_3 10.75, Li_2O 16.30, MgO 4.53, ZnO 3.00, K_2O 1.29, P_2O_5 1.28; (ii) oxide mixture obtained by thermal treatment of a gel formed during the mixed hydrolysis of metallorganic compounds of formula: $Ce(C_5H_7O_2)_3 \cdot xH_2O$ and $Zr(C_4H_9O)_4$.

In the first case the β-eucryptite/β-spodumene phase transition was followed and recorded. In the second case the X-ray line broadening was studied, as a function of the thermal treatment, with reference to a crystalline phase made of a tetragonal structured solid solution of the system: 0.84 ZrO_2–0.16 CeO_2.

2. Experimental details

2.1. Samples preparation

The glass chosen for the fibre production was obtained starting from pure chemical raw materials mixed in a platinum alloy crucible which was brought up to 1450° C and kept under a stirring action for two days. The fluid glass was poured and quenched to be broken down into small fragments. The latter were used to feed the fibre spinning apparatus described elsewhere [1]. Fibres with a mean diameter of about 15 μm were made. They were checked under a polarizing microscope and found to be clear and homogeneous.

For the preparation of the second material, the necessary amount of the metallorganic precursors, Ce(III)2-4-pentanedionate and Zr-tetra-*n*-butoxide, calculated on the basis of their actual cation concentration, were dissolved in an anhydrous ethanol solution. This latter was heated at a simmering temperature in a round bottom, two-necked flask equipped with a stirrer and reflux condenser. The excess ethanol was distilled off and the viscous

---

*To whom correspondence should be addressed.

0022–2461/83 $03.00 + .12

brown liquid was added of a certain amount of water to ensure complete hydrolysis. Gelling could take place in a short time. The semi-solid mass was left to dry overnight on a metal pan at 180°C.

2.2. Differential thermal analysis

Differential thermal analysis (DTA) was carried out with a Netzsch apparatus using the following experimental conditions: heating rate $10° \text{min}^{-1}$; sensitivity, 0.05 mV; sample weight, 200 mg/ 200 mg Al_2O_3; crucibles, platinum of 0.3 ml.

2.3. High temperature X-ray attachment

The description of the high temperature chamber, here employed, was published by Spinolo *et al.* [2] who are the originators.

The furnace is driven by a Leeds and Northrup three action current-adjusting type (CAT) controller in connection with a silicon rectifier power unit. Two thermocouples are employed: the one leading to the control unit is positioned in the furnace close to the heating wire; the other is inserted in a hole drilled from the bottom of the metal block, constituted by nickel, up to about 0.1 mm below the lower surface of the sample for the precise measurement of its temperature. The maximum temperature which the sample can reach is about 1000° C with a total accuracy of the system equal to ± 2° C. The precision is much higher: as an example, a typical result of some twenty measurements during about 2 h near 520° C shows a standard deviation of 0.2° C [2].

A Philips vertical diffractometer, the Cu$K\alpha$ Ni-filtered radiation and a scintillation detector with pulse-height discrimination were used. The calibration of the 2θ angular position was performed using a standard ZnO powder sample at the same experimental conditions. The alignment of the sample holder placed inside the chamber lid is easy and well repeatable in case of sample change.

In the study of β-eucryptite/β-spodumene transition the X-ray diagrams were recorded in the 2θ range between 14 and 30° using a scanning speed of $1° \text{min}^{-1}$. For the X-ray line broadening analysis of the zirconia–ceria solid solution only the 111 peak could be investigated. In this case a speed of $0.25° \text{min}^{-1}$ was employed.

3. Results and discussion

3.1. Glass–ceramic fibres

At first, the thermal evolution, i.e. the devitrification of the glass fibres was investigated by means of DTA and XRD (X-ray diffraction) standard equipments. The fibres were suitably powdered.

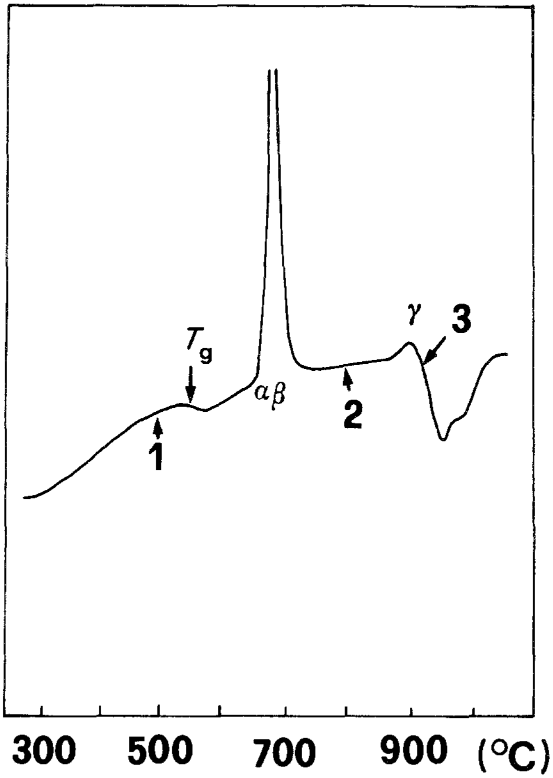

Figure 1 Differential thermal analysis (DTA) curve of glass fibres. The Greek symbols correspond to the crystalline phases reported in Fig. 2.

Fig. 1 shows the DTA curve of the glass fibres. It is characterized by a small endothermic effect at about 560° C, which is due to the glass transition and identified as the T_g temperature. This effect is followed by a strong exothermic peak at about 680° C due to the primary phase crystallization. Another small exothermic peak has been found at 900° C, before the endothermic sequence at 975° C.

Three points, reported in Fig. 1 as 1, 2 and 3, have been chosen to check for phase crystallization or reaction in this glass. As shown in Fig. 2, the phases found at the temperatures reported in the DTA trace, are Li_2MgSiO_4, $LiAlSiO_4$ (β-eucryptite) and $LiAlSi_2O_6$ (β-spodumene).

Beta-eucryptite is the primary phase found at about 680° C. With the present methods the Li–Mg–silicate has been detected at about the same temperature range. Its presence is based on diffraction peaks of weak intensity and of not very precise position. Upon further heating, between 870 and 925° C, the β-eucryptite phase transforms to a β-spodumene structure. The following endo-

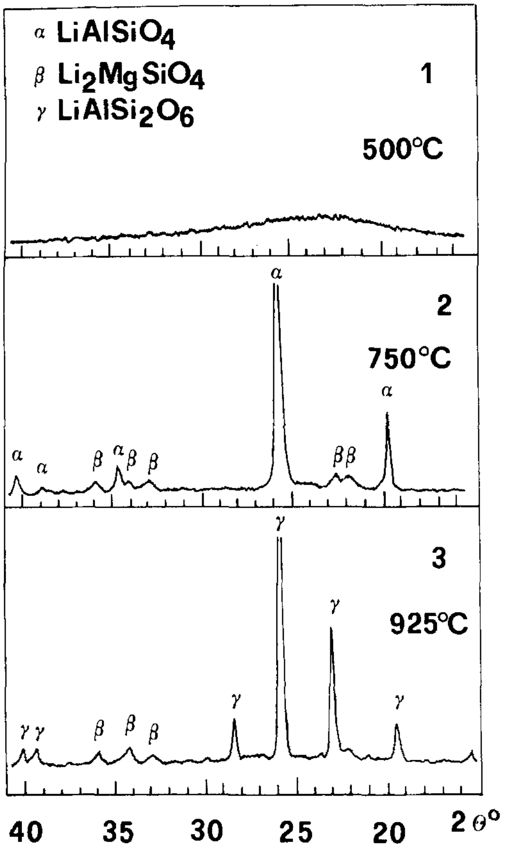

Figure 2 X-ray diffraction patterns of the fibres, after heating and quenching at the temperatures corresponding to the numbers indicated in the DTA curve of Fig. 1.

thermic peaks are probably due to the decomposition of the newly-formed phases or the softening of the remaining glass, because at 975° C the fibres are aggregated together. The formation of these crystalline phases is in agreement with previous observations on similar glass compositions which had been brought to devitrification, like the ones reported by Doherty *et al.* [3]. In the composition of this latter system TiO_2 (4.75 wt%) was present also, and the β-eucryptite/β-spodumene transition took place between 975 and 1025° C, i.e. at a temperature higher by 100° C than the one observed in the present system.

Since in several mass glassy systems (as opposed to fibre glassy systems) the β-eucryptite/β-spodumene transition was found to be very fast, as noted by Skinner and Evans [4] as well as by Doherty *et al.* [3], in this work we planned to follow the above mentioned transition by using the previously described high temperature chamber. In fact, it was not possible to obtain by quenching a XRD pattern in which both β-eucryptite and β-spodumene were present together.

Fig. 3 shows some meaningful XRD patterns directly obtained at high temperature within the 865 to 930° C temperature range. Each diffractogram started after an isothermal stage of 1 h at each temperature investigated, except for the one which was recorded at 880° C after 10 min. The wt % of β-eucryptite and β-spodumene were calculated as a function of temperature averaging two sets of complementary experimental data directly obtained from the relative X-ray intensities of (1 0 0) β-eucryptite and (1 0 2) β-spodumene reflections, respectively. In all the present XRD diagrams the intensity of the strongest peak appears nearly constant, independently on the temperature investigated. This fact shows that the X-ray intensities can be directly compared to each other in all the patterns investigated if we assume that the effect of temperature on XRD intensity is negligible in the present study ($\Delta T_{\mathrm{maximum}} = 65°$ C) and that no preferred crystal orientation is present.

TABLE I Percentages (wt%) of β-eucryptite and β-spodumene and related unit cell parameters, as functions of the thermal treatment

Temperature investigated (° C) ± 2	β-eucryptite (wt%) ± 5	β-spodumene (wt%) ± 5	β-eucryptite unit cell parameters		β-spodumene unit cell parameters	
			a_0 (nm) ± 0.002	c_0 (nm) ± 0.002	a_0 (nm) ± 0.002	c_0 (nm) ± 0.002
865 (1 h)	100	0	0.517	1.093	–	–
880 (1 h)	47	53	0.517	1.093	0.750	0.915
900 (1 h)	20	80	n.d.*	n.d.	0.750	0.915
910 (1 h)	15	85	n.d.	n.d.	0.750	0.915
930 (1 h)	0	100	–	–	0.750	0.915
880 (10 min)	64	36	0.517	1.093	0.750	0.915
Quenching from 750° C	100	0	0.521	1.094	–	–
Quenching from 925° C	0	100	–	–	0.744	0.914

*n.d. – no data.

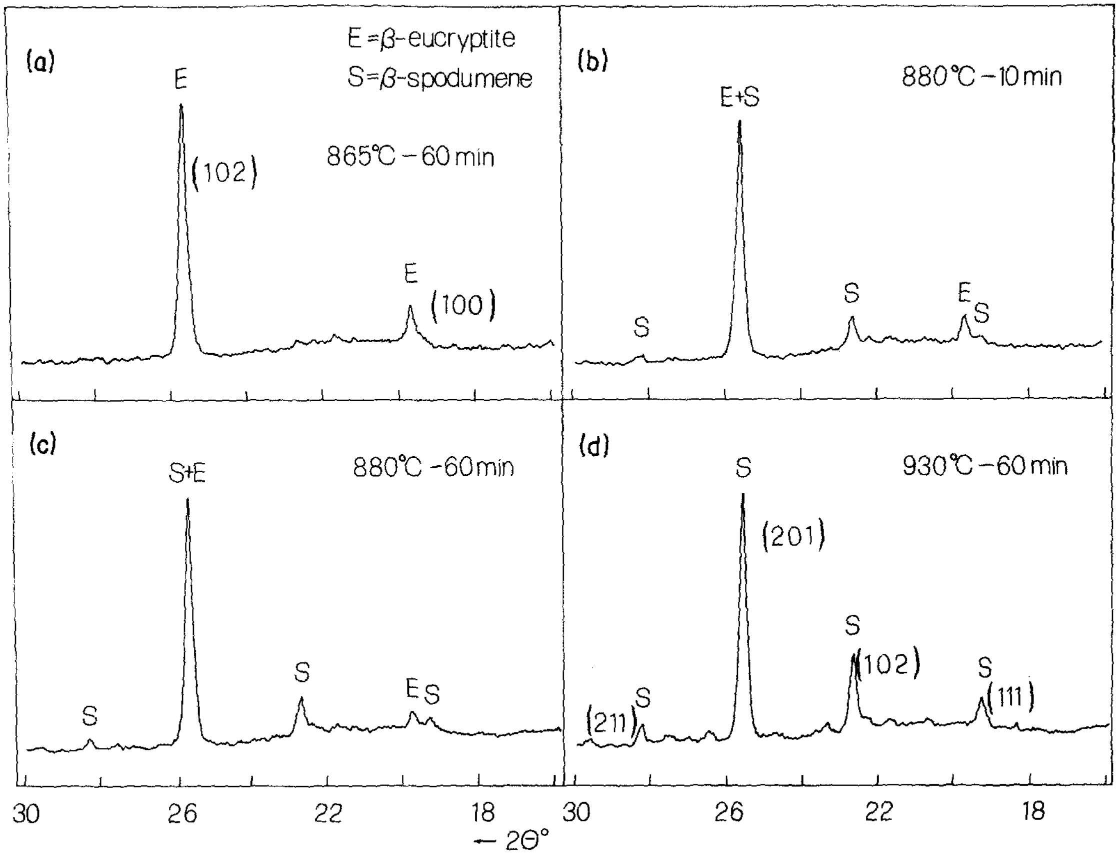

Figure 3 X-ray diffraction patterns of slightly powdered glass fibres, taken *in situ* by means of the high temperature attachment, within the 865 to 930° C range.

The so-obtained percentages are reported in Table I, where the unit cell parameters are also indicated. Fig. 4 shows both the trend of the amount of variation of the two phases involved, as a function of the temperature investigated, and the trend of increasing β-spodumene content during the isothermal stage at 880° C, as a function of time.

The hexagonal unit cell edges of pure β-eucryptite (space group $C6_22$) are reported in the literature to be equal to $a_0 = 0.527$ nm and $c_0 = 1.125$ nm [5] or to $a_0 = 0.5245$ nm and $c_0 = 1.120$ nm [6], whereas the pure β-spodumene tetragonal unit cell (space group $P4_32_12$) is quoted as follows: $a_0 = 0.7533$ nm, $c_0 = 0.9154$ nm [4] or $a_0 = 0.7541$ nm, $c_0 = 0.9156$ nm [7]. As indicated in Table I, the unit cell directly found at high temperature for β-eucryptite is somewhat lower than that reported in the literature, especially for the c_0 parameter, whereas the β-spodumene unit cell data turn out to be much closer to the values related to the stoichiometric compound. The unit cell shrinkages, here calculated for both the crystalline phases under investigation, point out that the first crystallized phase is surely an eucryptite–silica solid solution based on the β-eucryptite hexagonal structure and that the second phase is probably a solid solution of β-spodumene with silica, having a tetragonal structure. This agrees with the structure data reported by Roy [8], Skinner and Evans [4] and Keat [9]. Moreover, a previous paper by Hatch [10] showed, in a phase equilibrium study of lithia–alumina–silica system, the presence of β-eucryptite as well as of β-spodumene solid solutions with silica.

Thus, it is possible to conclude that the crystallization of the glassy phase of composition intermediate between pure eucryptite and pure spodumene starts firstly with a hexagonal β-eucryptite like structure (solid solution), to be subsequently transformed, at an adequate temperature, to a tetragonal β-spodumene structure. This observation also agrees well with the existence of solid solutions between β-eucryptite and β-spodumene, as shown by Hatch [10] and by Roy *et al.* [11].

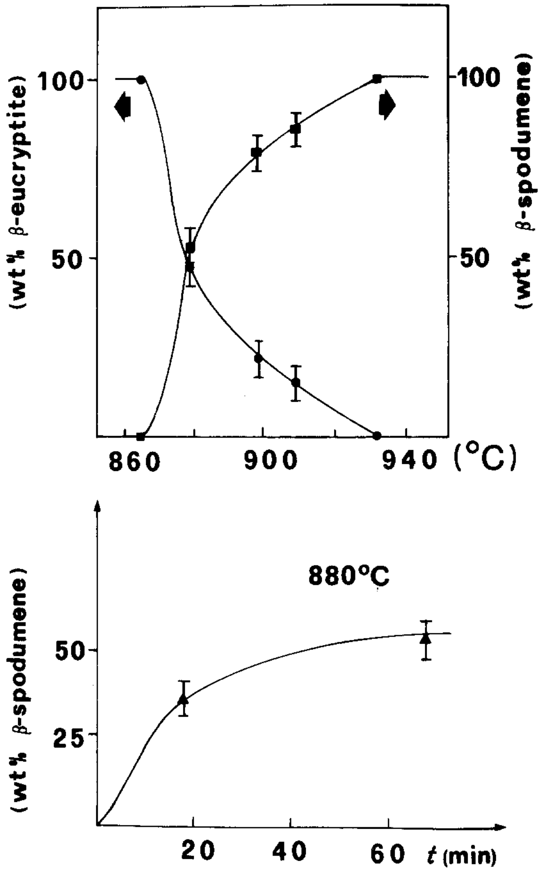

Figure 4 Variation of the wt% amount of β-eucryptite and β-spodumene as a function of temperature and time.

The possibility of replacing one aluminium plus one lithium atom by one silicon atom is well known in the tetragonal β-spodumene structure until the pure tetragonal silica, named keatite [9], is obtained. Beta-spodumene can be considered as a stuffed silica structure where lithium atoms progressively fill the available interstices. In the present glass–ceramic system we have shown that the phase inversion goes from a compound richer in lithium and aluminium, such as β-eucryptite, towards a compound less rich in lithium and aluminium, such as β-spodumene. The structures of these two compounds are similar which is shown by the angular closeness of some peaks in their X-ray patterns (for example the strongest peak is practically coincident in the solid solutions). As a result of these structure investigations, it can be easily explained that the heat involved in this transition is rather small, as shown by the second DTA exothermic peak in the curve of Fig. 1, owing to the fact that extended movements of ions are not required to occur, changing from one structure to the other.

3.2. ZrO_2–CeO_2 solid solution prepared from metallorganic precursors

As an illustration of the whole set of measurements, Fig. 5 shows four diffractograms of the zirconia–ceria tetragonal solid solution recorded at 460, 620, 776 and 944° C, respectively, after two hours at each temperature investigated, in order to be close to the thermodynamic equilibrium of the system.

The average crystallite size, measured perpendicularly to the (1 1 1) reflecting planes, L_{111}, has been obtained by applying the well known Scherrer Equation:

$$L_{111} = \frac{K\lambda}{\beta \cos \theta_{111}}$$

where β is the "pure" or corrected line width (or breadth), λ is the wave-length of the Cu$K\alpha$ radiation and K is a constant which is close to 0.9 when β is measured as half-maximum width ($\beta_{1/2}$), whereas it is close to 1.1 when the integral breadth (β_i) is used. In both cases the K values refer to octahedrally shaped crystallites [12].

Since the observed (non corrected) X-ray line widths are large enough and the $K\alpha$ doublet separation small enough so that the doublet correction can be neglected, only the correction for instrumental broadening has been carried out, using the narrow X-ray reflections of a polycrystalline ZnO standard specimen irradiated on the same experimental conditions used for the solid solution samples. The X-ray 1 1 1 line profile, due to the sample heated at 944° C, was found to be very close to a Lorentzian square (or modified) function. In fact, from a least square calculation, based on a set of about thirty experimental points, the observed profile was fitted well with a Pearson VII analytical function [13] having an exponent value close to 2. For this kind of profiles a correction curve reported by Tekiz and Legrand [14] is very suitable, so it has been employed here.

In Fig. 6 it is possible to see the trends of L_{111} obtained either from $\beta_{1/2}$ or β_i as functions of the temperature investigated. The two trends are similar to each other, showing that, starting from about 650 to 750° C, the crystal growth is enhanced as a function of the temperature, with respect to the linear increase shown in the range between 219 and 650° C. A question can arise in connection with a possible influence of the thermal diffusion scattering (TDS) upon the X-ray line breadths [15]. In order to evaluate experimentally

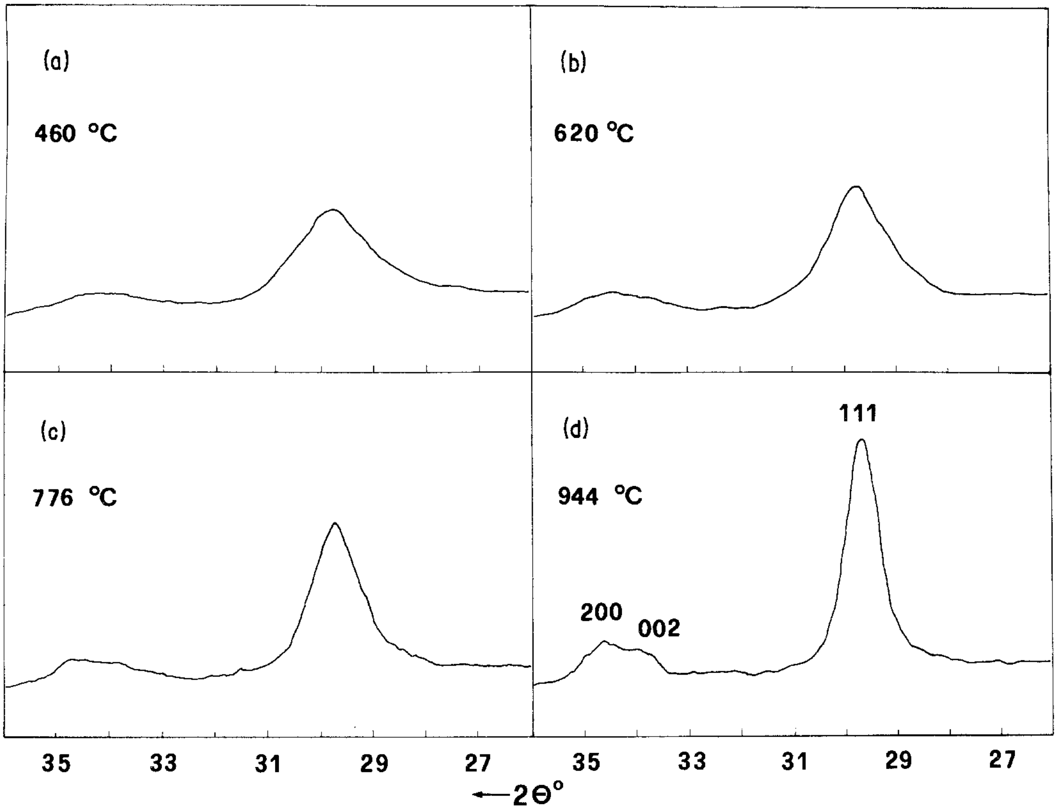

Figure 5 X-ray 1 1 1 reflection of the zirconia–ceria solid solution recorded at various temperatures. In the last diffractogram the 0 0 2–2 0 0 tetragonal doublet is evident.

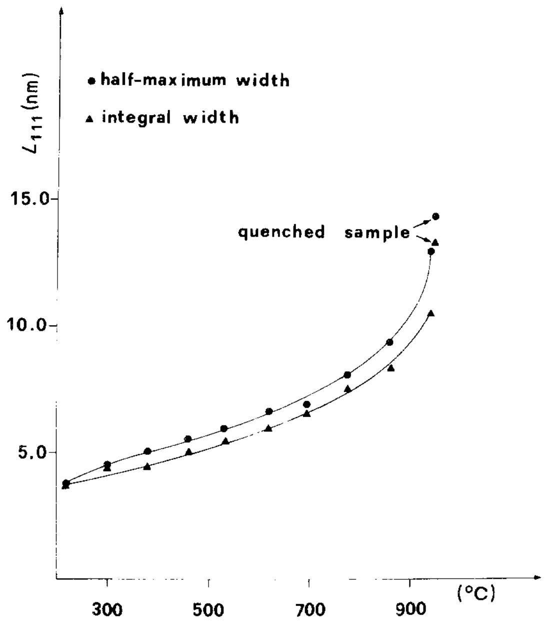

Figure 6 Trends of the L_{111} crystallite sizes, obtained from either half-maximum or integral width, as functions of the temperature, for the zirconia–ceria solid solution. The relative error is indicated in Fig. 7 (± 1 nm).

this effect we have examined at room temperature the sample after having quenched it from 944° C. A slight decrease has been noted in the order of about 10%, for either $\beta_{1/2}$ or β_i corresponding to a slight increase in crystallite size, as shown in Fig. 6. Therefore, it is possible to conclude that systematic errors introduced by TDS are tolerable for the purpose of this research work, in the temperature range here investigated, taking also into account that the material examined has a very high melting point (about 2700° C). In Fig. 7 a kinetic curve for the L_{111} growth at 944° C is displayed.

In Fig. 8 the trend for the d_{111} interplanar distance increase, as a function of temperature, is shown. For comparison purposes, the d_{111} values of pure tetragonal zirconia and pure cubic ceria are equal to 0.2957 nm [16] and 0.3124 nm [17], respectively. Also for this parameter a significant enhancement can be noted after 600 to 650° C. From these data an average thermal expansion coefficient, α, of about $10 \times 10^{-6}\,(\mathrm{K}^{-1})$ was obtained for temperatures in the range 600 to 900° C.

All the present observations agree with the

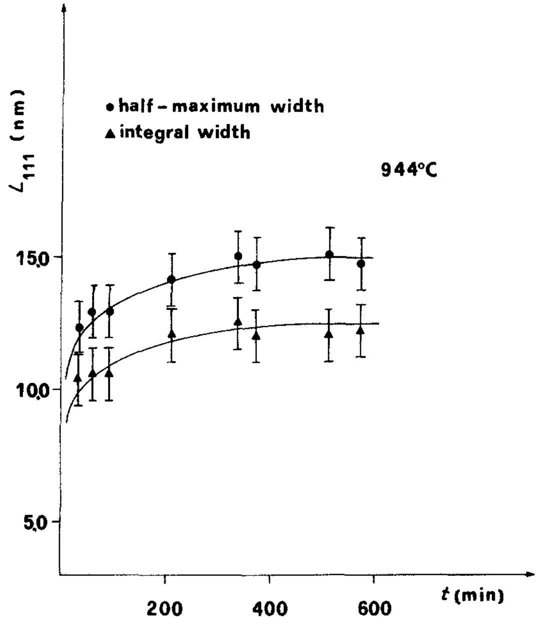

Figure 7 Variation of L_{111} at 944° C as a function of time.

results recently reported by Meriani and Soraru [18] who showed that the reactivity of the "as gelled" precursors was very high, while the sintering ability was poor. A better sinterability was presented by "calcined-gel" precursors for which a firing treatment at about 550° C assured a complete carbon burn out and delivered a bright yellow powder which could be pressed down into pellets of about the same green density obtainable by an oxides mixture made up in a conventional way. The higher sintering ability shown by the "calcined-gel" oxides can be paralleled with the present structural data which show that, at temperatures higher than 600 to 650° C, the crystal growth and the crystal thermal expansion of the zirconia–ceria solid solution become meaningfully higher than those presented at lower temperatures.

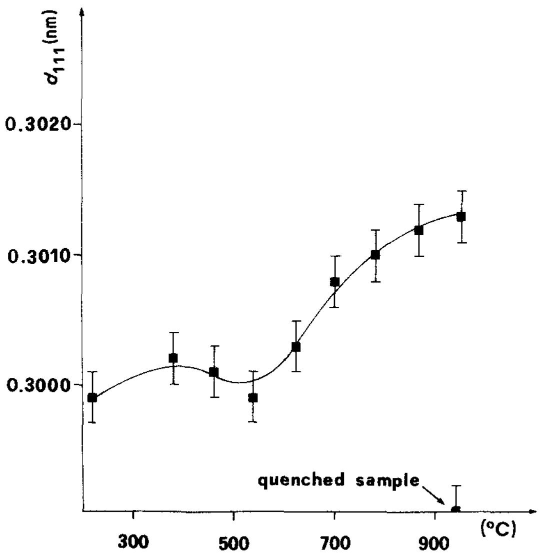

Figure 8 Variation of the interplanar distance, d_{111}, as a function of temperature.

Acknowledgements

We thank the Italian Research Council (CNR, Roma) for the financial support obtained for this work in the "Progetto Finalizzato Chimica Fine e Secondaria – Sottoprogetto Metodologie" research programme. Assistance in the experimental work by D. Rudello and R. Zuliani is gratefully acknowledged.

References

1. A. BENEDETTI, G. COCCO, G. FAGHERAZZI, B. LOCARDI and S. MERIANI, *J. Mater. Sci.* **18** (1983) 1039.
2. G. SPINOLO, V. MASSAROTTI and G. CAMPARI, *J. Phys. E: Sci. Instrum.* **12** (1979) 1059.
3. P. E. DOHERTY, D. W. LEE and R. S. DAVIS, *J. Amer. Ceram. Soc.* **50** (1967) 77.
4. B. J. SKINNER and H. T. EVANS Jr, *Amer. J. Sci.* **258A** (1960) 312.
5. H. G. F. WINKLER, *Acta Cryst.* **1** (1948) 27.
6. T. ISAACS and R. ROY, *Geochim. Cosmochim. Acta* **15** (1958) 213.
7. CHI-TANG LI and D. R. PEACOR, *Z. Kristallogr.* **126** (1968) 46.
8. R. ROY, "Symposium on Nucleation and Crystallization in Glasses and Melts" (American Ceramic Society, Columbus, Ohio, 1962) p. 39.
9. P. KEAT, *Science* **20** (1954) 328.
10. A. HATCH, *Amer. Mineral.* **28** (1943) 471.
11. R. ROY, D. M. ROY and F. F. OSBORN, *J. Amer. Ceram. Soc.* **33** (1950) 152.
12. J. I. LARGFORD and A. J. C. WILSON, *J. Appl. Cryst.* **11** (1978) 102.
13. M. M. HALL Jr, V. G. VEERARAGHAVAN, H. RUBIN and P. G. WINCHELL, *ibid.* **10** (1977) 66.
14. J. TEKIZ and C. LEGRAND, *Compt. Rend.* **261** (1965) 1247.
15. B. E. WARREN, "X-ray Diffraction" (Addison-Wesley Publ. Co., Reading, Massachussets, 1969) p. 193.
16. C. A. SORRELL and C. C. SORRELL, *J. Amer. Ceram. Soc.* **60** (1977) 495.
17. Powder diffraction file, JCPDS 1974; Inorganic volume no. 4-0593.
18. S. MERIANI and SORARÙ, Proceedings of the 5th CIMTEC Congress, edited by P. Vincenzini (Lignano, Italy) in press.

Received 3 August
and accepted 20 October 1982